Graphene veils: A versatile surface chemistry for sensors

Shawn P. Mulvaney[1], Rory Stine[2], Nina C. Long[2], Cy R. Tamanaha[1], and Paul E. Sheehan[1]
[1]US Naval Research Laboratory, Washington, DC and [2]Nova Research, Inc., Alexandria, VA

BioTechniques 57:21-30 (July 2014) doi 10.2144/000114188
Keywords: biosensor; graphene oxide; surface chemistry; coating; film

Thin spun-coat films (~4 nm thick) of graphene oxide (GO) constitute a versatile surface chemistry compatible with a broad range of technologically important sensor materials. Countless publications are dedicated to the nuances of surface chemistries that have been developed for sensors, with almost every material having unique characteristics. There would be enormous value in a surface chemistry that could be applied generally with functionalization and passivation already optimized regardless of the sensor material it covered. Such a film would need to be thin, conformal, and allow for multiple routes toward covalent linkages. It is also vital that the film permit the underlying sensor to transduce. Here we show that GO films can be applied over a diverse set of sensor surfaces, can link biomolecules through multiple reaction pathways, and can support cell growth. Application of a graphene veil atop a magnetic sensor array is demonstrated with an immunoassay. We also present biosensing and material characterization data for these graphene veils.

For sensors, the method of transduction rarely limits performance, as seen in the multiple techniques that can detect single molecules (1–3). Rather, sensors commonly fail due to the interface between the sensor and sample. This is particularly true in biosensing, where complex matrices such as blood, urine, saliva, and sputum typically degrade the limit of detection by one to four orders of magnitude, or cause outright failure (4). The literature on biosensor surface preparation is vast—clear documentation of the time, effort, and resources poured into perfecting surface chemistries (5–11).

An overwhelming difficulty in biosensing is that each sensor material must be addressed separately (9–14). That is, a surface chemistry that works for gold will not work for silicon or gallium nitride or any other technologically relevant material. There would be enormous value in separating the problem of how a molecule is sensed from the problem of how to chemically functionalize and passivate that sensor. An ideal surface chemistry would produce a film thin enough to keep the biomolecules close to the sensing element, be conformal, and allow for multiple routes toward covalent linkages. Moreover, the film must be sufficiently robust so that it remains intact during washing and sensing, and must not interfere with the transduction mechanism.

The creation of thin conformal films has most often been accomplished with self-assembled monolayers (SAMs) (9,10). Prominent examples are silane films polymerized on silicon dioxide, alkanethiol films formed on gold surfaces, and isothiocyanate films on platinum surfaces. While effective, these functionalization pathways are highly material dependent and therefore lack generality. More general approaches can be found in layer-by-layer polymer films, parylene coatings, and Janus membranes. Layer-by-layer films are formed by the electrostatic addition of polymers with opposite polarity (15,16). These films are typically tens to hundreds of nanometers thick, and the initial layer deposition depends on and influences the sensor substrate material. Ultimately layer-by-layer films hold promise for some sensing applications, but their thickness creates difficulties, and surface charge interferes with transduction for techniques such as surface plasmon resonance (SPR) and field effect transistors (FETs).

An alternative approach that is agnostic to the sensor material is the use of parylene films. Parylene coatings are self-initiating polymer films made with vapor deposition techniques (17). Their bioapplication is well-established, and they have found significant use as the nonfouling coating on implanted medical devices. The great advantage of parylene coatings is that these nonfouling films offer multiple pathways toward covalent linkages by using monomers with different pendant groups. However, most parylene films are hundreds of nanometers in thickness; even the

METHOD SUMMARY

Five technologically important and diverse substrates were coated with a thin, conformal graphene oxide (GO) film, subsequently functionalized with an array of chemistries, and then successfully used in immunoassays and nucleic acid hybridization assays. We further demonstrate that graphene veils can mask the substrate material from the biological material with the growth of human mesenchymal stem cells atop what are otherwise inhospitable substrates.

thinnest reported parylene films are ~10 nm thick, which already approaches the Debye length at which FET sensors fail to transduce. Furthermore, the fabrication of parylene films requires highly specialized equipment not common to the typical chemistry laboratory.

A thinner and truly surface-agnostic alternative is the use of Janus membranes created by Turchanin and co-workers (18–20). Janus membranes are formed by creating a thiolated SAM on a gold surface and then crosslinking aromatic constituents of the film with UV light. Based on the molecule used to make the SAM, the Janus membrane can have orthogonal chemistry on each face and form pores of controlled size. Most importantly, the Janus membranes can be removed from the gold surface, producing ~1 nm thick, freestanding films that can be transferred onto any sensor material. While an elegant solution, the transfer process requires multiple steps, including the addition of a photoresist, acid digestion of the gold film, transfer, removal of the photoresist, and additional intermediate cleaning steps.

A new material providing a versatile chemistry is graphene, which, since its recent development in 2004 and subsequent recognition with the Nobel Prize, has been a subject of intense study in many fields (21). With regards to sensing, graphene's excellent electronic properties have inspired its use in FETs, electrochemical sensors, and as the quenching partner in Förster resonance energy transfer (FRET) systems (22,23). More recently, graphene has been used in hybrid applications, such as observation of electrochemical events with SPR (24–27). In these applications, graphene is deposited over gold films and acts as an electrode, enabling the products of electrochemical reactions to be monitored with SPR.

Here we expand upon the idea of hybrid graphene surfaces to demonstrate that graphene oxide (GO) films can be placed on a wide variety of surfaces, including those notoriously difficult to functionalize, such as III-V semiconductors (13,28). While there has recently been subtle work showing the chemical interplay between single layer graphene and the underlying substrate (29–32), the goal here is not to study such substrate effects but rather to produce a chemical veil that effectively masks the substrate while being transparent to the transduction mechanism. Moreover, it was critical that we do so in a simple, inexpensive, and routine manner. Consequently, the same base surface chemistry was applied to all substrates in this study to enable multiple pathways toward covalent coupling. The generality of our approach was demonstrated with both nucleic acid and protein bioassays; moreover, graphene veils made possible in vitro studies by supporting cell growth and function on these same sensor substrates. Finally, these thin graphene veils were fully characterized and were also demonstrated to work in complex matrices.

Materials and methods

All reagents were used as acquired unless otherwise noted. Ethylenediamine (EDA), acetone, powdered graphite, sulfuric acid, potassium permanganate, sodium nitrate, hydrogen peroxide, sodium chloride, sodium citrate, sodium phosphate monobasic, sodium phosphate dibasic, ricin A chain toxoid (RCA), mouse anti-MYC antibody, and methanol were purchased from Sigma-Aldrich (St. Louis, MO). Succinimidyl 4-hydrazinonicotinate acetone hydrazine (SANH), succinimidyl 4-formylbenzoate (SFB), N-hydroxysulfosuccinimide (NHS), 1-Ethyl-3-[3-dimethylaminopropyl]carbodiimide hydrochloride (EDC), and all magnetic beads [M280 Dynabeads- sheep anti-mouse; sheep anti-rabbit, steptavidin, or oligo $(dT)_{25}$] were purchased from Thermo-Fisher Scientific (Waltham, MA). Solulink (San Diego, CA) supplied HyNIC-MYC peptide reagents. Rabbit anti-RCA and biotinylated mouse anti-RCA were purchased from Tetracore (Rockville, MD). Biotinylated mouse IgG was obtained from KPL (Gaithersburg, MD). All oligonucleotide sequences were custom synthesized and purified with HPLC by IDT Technologies (Coralville, IA). Human mesenchymal stem cells (hMSC), mesenchymal stem cell growth media (MSCGM), MSCGM supplemental kit, penicillin, and streptomycin were purchased from Lonza (Walkersville, MD). Lonza's MSCGM supplement kit includes growth supplement, L-glutamine, gentamicin sulfate, and amphotericin-B. Calcein AM, ethidium homodimer (EthD-1), and trypsin EDTA were purchased from Life Technologies (Grand Island, NY). Corning Incorporated (Corning, NY) polystyrene tissue culture plates and flasks were used for all cell culture.

Graphene veil

GO was prepared via the Hummers method (33) using powder that was first dissolved in water (2 mg/mL). GO solution was spin coated onto the desired surface, one drop at a time, under flowing N_2 (34). The deposited GO films were then annealed at 110°C for 1 h to remove water. As measured by AFM, the resulting films were ~4 nm in thickness.

Amination of graphene veils

GO veils were reacted with 1% EDA in acetone for 1 h. Unreacted EDA was removed from the surface by washing with acetone and water, and lastly blow drying in an N_2 stream (34,35). XPS, ATR-FTIR, and Raman data supporting the reaction of EDA with graphene have been published previously (35).

Conjugation of aminated graphene veils

Aminated graphene veils can be reacted via a variety of conjugation pathways. Here, two pathways were demonstrated. First, amine to amine linking was accomplished via the hydrazone reaction facilitated by the crosslinkers SFB and SANH. SFB was reacted with the aminated graphene veil at pH 7.2. SANH was reacted with either aminated-oligonucleotide strands or proteins at pH 7.2, depending on the experiment. Finally, the SANH conjugated biomolecules were grafted onto the SFB conjugated graphene veil at pH 5.5.

The second functionalization pathway demonstrated was reaction of the aminated graphene veil with 2 mM EDC and 5 mM NHS in pH 7.2 phosphate buffer for 15 min. The EDC/NHS solution was aspirated and replaced with a 1 mg/mL solution of neutravidin (NA) in pH 7.2 phosphate

Table 1. Oligonucleotide sequences for nucleic acid hybridization assays.

Substrate	Probe	Sequence (5´-3´)
GaN	capture 1	amine-TCTAGGCTGACGGATAACCGAAGA
	target 1	TTTTTTCTTCGGTTATCCGTCAGCCTAGATAACCGAGCAAGACACTTGTACAGCAGCAAGTGATTGTTGCAGTCAACCTATCCACTGGGCTCCCAGG
	label 1	GCTGTACAAGTGTCTTGCTCGGTT-biotin
InAs	capture 2	amine- AACAAGTGTTTATATATTCGGTTA
	target 2	TTTTTTATCGGTTGGCGTTAAACACGCTAACCGAATATATAAACACTTGTTTAAGCTCAGGTGATTGTTGCAGTCAACCGATCCACTGGGAGCCGAATTCTTCCCAGTT
	label 2	TGACTGCAACAATCACCTGAGCTT-biotin
polystyrene	capture 3	GCTGTACAAGTGTCTTGCTCGGTT-biotin
	target 3	TTTTTTCTTCGGTTATCCGTCAGCCTAGATAACCGAGCAAGACACTTGTACAGCAGCAAGTGATTGTTGCAGTCAACCTATCCACTGGGCTCCCAGG
	label 3	AAAAAAAAAAAAAAAAAAAAAAAAATCTAGGCTGACGGATAACCGAAGA

buffer for 2 h. Finally, the surface was rinsed with water and dried in an N_2 stream.

Conjugation of native graphene veils

The polystyrene surface was coated with a graphene veil as described above. The surface was exposed for 2 h to a solution of 5 mM EDC and 1 µg/mL NA in 100 mM, pH 6.0, MES buffer. After conjugation, the veil was rinsed with water and dried in an N_2 stream. Finally, biotinylated DNA probes were spotted on the graphene veil.

Nucleotide hybridization assays

Graphene veils functionalized with oligonucleotide strands were hybridized with both a target strand and a label strand. The complementarity of the interaction resulted in the target strand hybridizing with both the surface-bound strand and the label strand such that terminal functionalization was oriented away from the graphene veil; specifically, for FFD assays performed atop GaN and InAs the biotin group and for the FFD assay performed atop polystyrene, the poly$(A)_{25}$ tail was facing away. Either steptavidin or oligo$(dT)_{25}$ conjugated M280 Dynabeads were then attached to the DNA hybrids. Excess beads were removed with controlled fluidic forces as described in detail in our previous papers (36,37). The GaN, InAs, and polystyrene surfaces were exposed to 1 of 2 different DNA sequences at 100 nM, 100 nM, and 1 µM target concentrations respectively. All sequences are listed in Table 1.

Peptide immunoassay

MYC peptide was attached to the graphene veil with a variation of amine-to-amine conjugation; HyNic is the equivalent of the SANH half when

reacting with SFB for surface functionalization. The SiO_2 substrate with peptide functionalized graphene veil was placed in a flow cell and exposed to 100 ng/mL mouse anti-MYC antibody for 5 min in stop flow. Flowing buffer removed the excess antibody and introduced sheep anti-mouse conjugated microbeads. The beads were allowed to settle for 3 min before application of controlled fluidic forces to remove nonspecifically attached beads.

RCA immunoassay

NA was attached to the graphene veil with SFB/SANH chemistry. Next, the surface was spotted with goat anti-RCA antibody. FFD assays were performed in 5 min stop flow steps with the addition of 100 ng/mL RCA toxoid in either buffer or 100% beagle serum, followed by 1 µg/mL mouse anti-RCA antibody. FFD immunoassay was completed with sheep anti-mouse microbeads.

IgG immunoassay

The magnetic microchip was coated with a NA coated graphene veil. Biotinylated mouse IgG antibody was spotted over a subset of sensors. The sensor chip was sealed in a flow cell and exposed to sheep anti-mouse microbeads. Following the FFD assay, the sensor chip was read magnetically in the cBASS prototype instrument and then removed for optical inspection.

Cell growth on graphene veil

hMSC cell cultures were initiated from frozen stocks and grown in 175 cm^2 tissue culture flasks for 1 week in MSCGM media that included growth supplements and antibiotics. Culture expansion was performed with trypsin release to seed six tissue culture flasks that were grown for an additional week's time.

SiO_2 and InAs substrates (~ 1 cm^2) were sterilized with ethanol, dried in an N_2 stream, and attached to the bottom of tissue culture dishes. hMSCs were released from the culture flasks with trypsin and then subcultured onto the tissue culture plastic and substrate materials at a density of 4500 cells/cm^2. Cells were grown at 37°C in a humidified incubator with 5% CO_2 for 3 weeks. Media was exchanged twice a week. Following three weeks of growth, all samples were exposed to a live/dead stain. The cells were stained with calcein AM and ethidium homodimer (EthD-1) for 1 h at 37°C. The stain was then exchanged with fresh growth media for imaging on a fluorescence microscope. Micrographs were collected immediately after staining at 10× magnification using the ex. 482 nm/em. 534 nm filter cube to image the calcein AM and the ex. 543 nm/em. 591 nm filter cube to image the EthD-1. Dual color images were created in Photoshop.

Results and discussion

The substrate–sample interface is critical to the success or failure of sensor technologies. Vast amounts of time, effort, and money have been expended in optimizing sensor surface chemistries (6–11), reflecting the fact that every sensor has its own material-dependent chemistry. Consequently, a generalizable surface chemistry that would be agnostic toward the underlying sensor materials is desirable. Optimization would only need to be done once, and any subsequent improvement would be equally applicable to all such coated sensors.

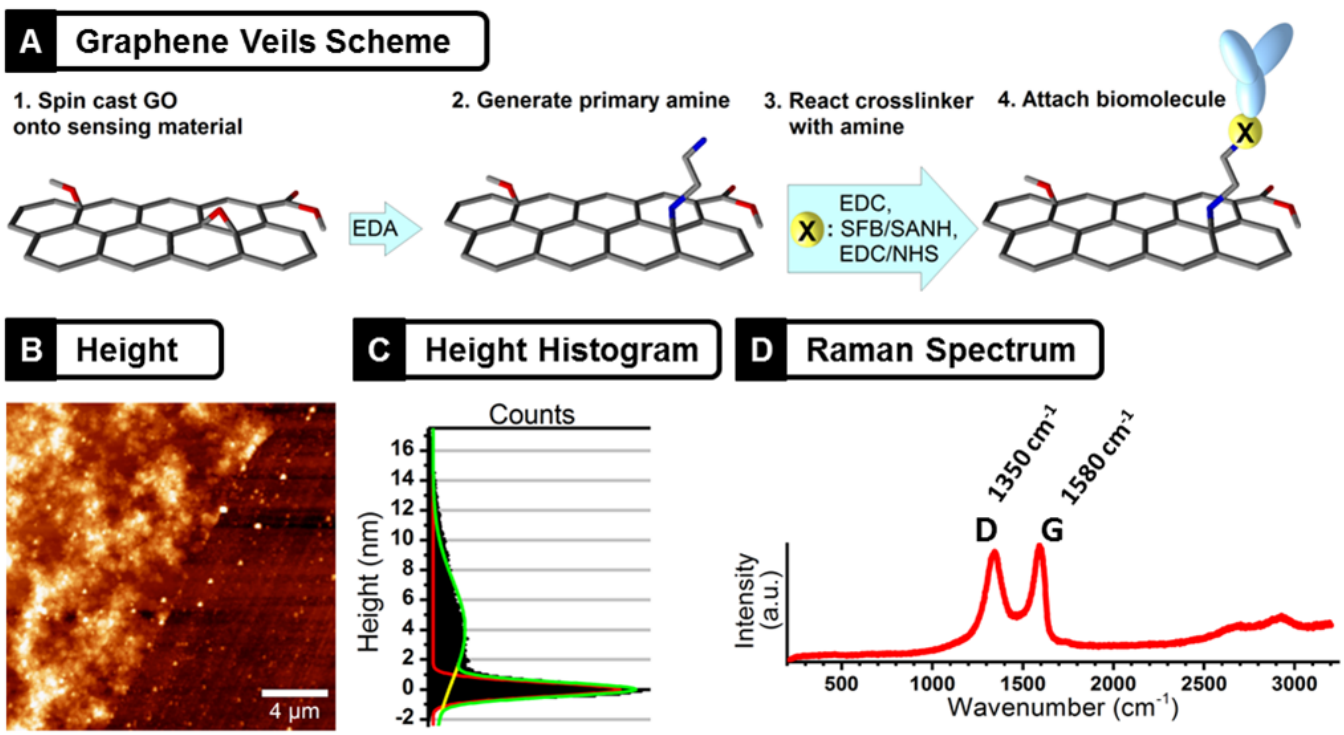

Figure 1. Characterization of graphene veils. (A) Scheme of graphene veil. Graphene oxide (GO) was spin cast atop a sensor material. The graphene veil was reacted with ethylenediamine (EDA) and amine reactive crosslinkers, and finally functionalized with biomolecules. (B) AFM topography of a GO film scratched (right side) to expose the substrate. (C) Height histogram showing the 3.98 ± 3.38 nm film thickness of the broad (yellow) GO peak. The narrower, more pronounced peak (red) is the substrate and was set to zero height. (D) Raman spectrum of a GO film showing the expected D and G band intensities with a D/G peak intensity of ~1.

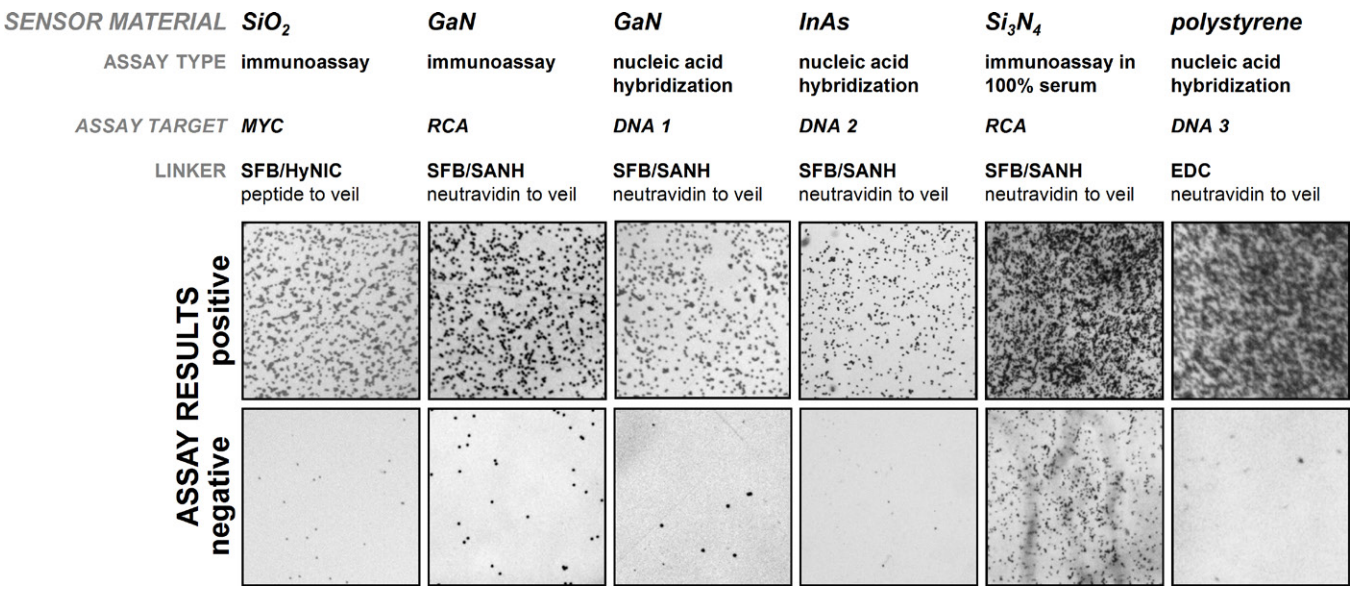

Figure 2. FFD sandwich immunoassays and DNA sandwich hybridization assays on graphene veils coating five diverse sensor materials. The assay type, assay target, and the linker used to attach the capture biomolecule to the graphene veil are listed for each column. The top row of positive results shows FFD assays where all components needed for bead capture are present. The bottom row of negative results shows FFD assays where only the target biomolecule was omitted.

Such a material would need to be thin, conformal, provide multiple pathways toward covalent linkages, and most importantly permit transduction by the underlying sensor.

Producing graphene veils requires only common laboratory techniques and no special equipment (Figure 1). While also commercially available, the GO used in this study was produced in our laboratory via the Hummers method (33), spin cast onto the substrate, and annealed to remove excess water and compact the film. The resulting conformal films were 3.98 ± 3.38 nm thick as measured by AFM (Figure 1, B and C) where the error is the standard deviation in the Gaussian fit of the film peak. The Raman spectra of the resulting films evidenced the expected G and D bands (1580 and 1350 cm^{-1}, respectively) indicative of GO, specifically the incorporation of oxygen in the form of epoxide, alcohol, and carboxyl groups (Figure 1D). The consistent Raman spectra across the substrate also demonstrated that we achieved a conformal coating of all surface features, including the nanostructures present in our group's bioFET sensors (34); on that sensor substrate, planar sensor areas are interspersed with 10 nm high gold contacts. Literature reports further indicate that GO films are good coatings for nanoarchitectures as shown by the conformal coating of nanoparticle agglomerates made from tin oxide nanoparticles, each ~15 nm in diameter (38) and the coating of TiO_2 nanocables, each 200 nm in diameter (39). We note that the ~5 nm GO coating observed on the TiO_2 nanocable is of a similar thickness to our graphene veils.

It has been demonstrated that the GO epoxide sites are spontaneously reactive with primary amines, and the addition of ethylenediamine (EDA) results in a facile amination (34). XPS, ATR-FTIR, and Raman data supporting the reaction of EDA with graphene have been published previously (35). Aminated GO films can then react with a wide range of commercial bioconjugation products that rely on succinimidyl chemistry. Figure 2 depicts assays using three different linkers taken from combinations of SANH, SFB, NHS, and EDC. Amine-to-amine coupling was achieved with the combination of SFB and SANH; each half links to a primary amine via a succinimidyl group and then crosslinks the two halves with hydrazone chemistry (40). Likewise, EDC by itself, or in combination with NHS, is a carboxyl-to-amine crosslinker (41).

Here we primarily use aminated graphene veils. The advantages are several-fold: First, the literature is replete with amine reactive chemistries, so much so that numerous commercial products have been developed for amine reactions. Second, amine groups are common in biology and therefore one of the most popular functional groups for conjugation reactions. Third, the reaction of EDA with GO is highly favorable and helps avoid issues of steric hindrance when attaching some biological entities directly to the 2-D surface. Lastly, should there be a need to reduce the GO film back to pristine graphene, the EDA chemistry is known to survive the harsh exposure to hydrazine (35). Nevertheless, the concept of a graphene veil does not have to use amine coupling; for example, a graphene veil with carboxyl linkage is also shown in Figure 2.

Critically, graphene veils must function reproducibly regardless of the substrate materials they coated. Figure 2 shows the results for fluidic force discrimination (FFD) assays performed on five diverse sensor materials. FFD assays (36,37) are sandwich-style assays that capture a target molecule between a capture agent tethered to the graphene veil and a second capture

agent tethered to a microparticle. Following biorecognition, a controlled fluidic force was applied to the bead labels that was strong enough to push off nonspecifically captured beads, but too weak to disrupt the specific interactions. Figure 2 shows results from both immunoassays and nucleic acid hybridization assays. The row of positive assay results shows beads captured on and bound to the graphene veil via biorecognition following FFD. The row of negative assay results shows the same surface when the assay target is missing and therefore specific biorecognition is not possible; FFD can remove the nonspecifically attached bead labels. For the silicon dioxide substrate, the MYC peptide was grafted onto the graphene veil with SFB/HyNIC chemistry, and an anti-MYC monoclonal antibody was detected. HyNIC is the commercial analog of SANH conjugated to the molecule, in this case the MYC peptide. The graphene veils atop the III-V semiconductor surfaces, GaN and InAs, were first functionalized with NA protein using SFB/SANH chemistry. NA functionalization offers two important advantages: it links to biotinylated biomolecules, and its net neutral charge reduces nonspecific binding. An immunoassay for ricin A chain toxoid (RCA) and DNA hybridization assays for 104 bp oligonucleotide targets were achieved on the III-IV semiconductor surfaces. Similarly, a graphene veil was added to a fourth material, silicon nitride, and a successful FFD assay for RCA was performed. Importantly, this assay was performed atop the graphene veil with the RCA target present in 100% beagle serum. The slightly higher background signal due to matrix effects (~10%) was expected and was consistent with previously published FFD assay results atop a glass slide using conventional surface passivation chemistries (36,37). Finally, a graphene veil was successfully added to a flexible plastic substrate, polystyrene. For this experiment, NA was covalently linked to the graphene veil through the native carboxyl groups using EDC as a crosslinker; there was no EDA intermediate layer present. A DNA hybridization assay for a 104 bp oligonucleotide target was then successfully performed.

We emphasize that biosensing requires exceptionally high quality surface chemistry since complex matrices lead to reduced sensitivity, fouling, and often outright failure of sensors (4). We demonstrated that both nucleic acid hybridization and immunoassays can be performed in either buffer or complex matrices. Notably, the background in the FFD assay for RCA in 100% serum was comparable to our previous results, meaning that the graphene veil added no significant background contribution when compared with an optimized, conventional surface chemistry. Moreover, the number of captured beads for each target concentration also agrees with our previous FFD assay results atop an optimized, conventional surface chemistry. Finally, the versatility of the graphene veil makes possible the addition of many passivation strategies, should one chose such additions. In addition to the neutrally charged NA coating we have demonstrated, the covalent attachment of polyethylene glycol (PEG), albumin, or other passivation entities can be completed via the described amine or carboxyl chemistry.

Delamination was not observed for graphene veils on any of the substrate materials tested. The robust nature of the graphene veil was demonstrated by our choice of a mechanically demanding assay. FFD assays are performed in a flow cell to enable the fluid to push on the beads and thereby to pull on the biomolecular interactions that connect them to the film. This lowers the

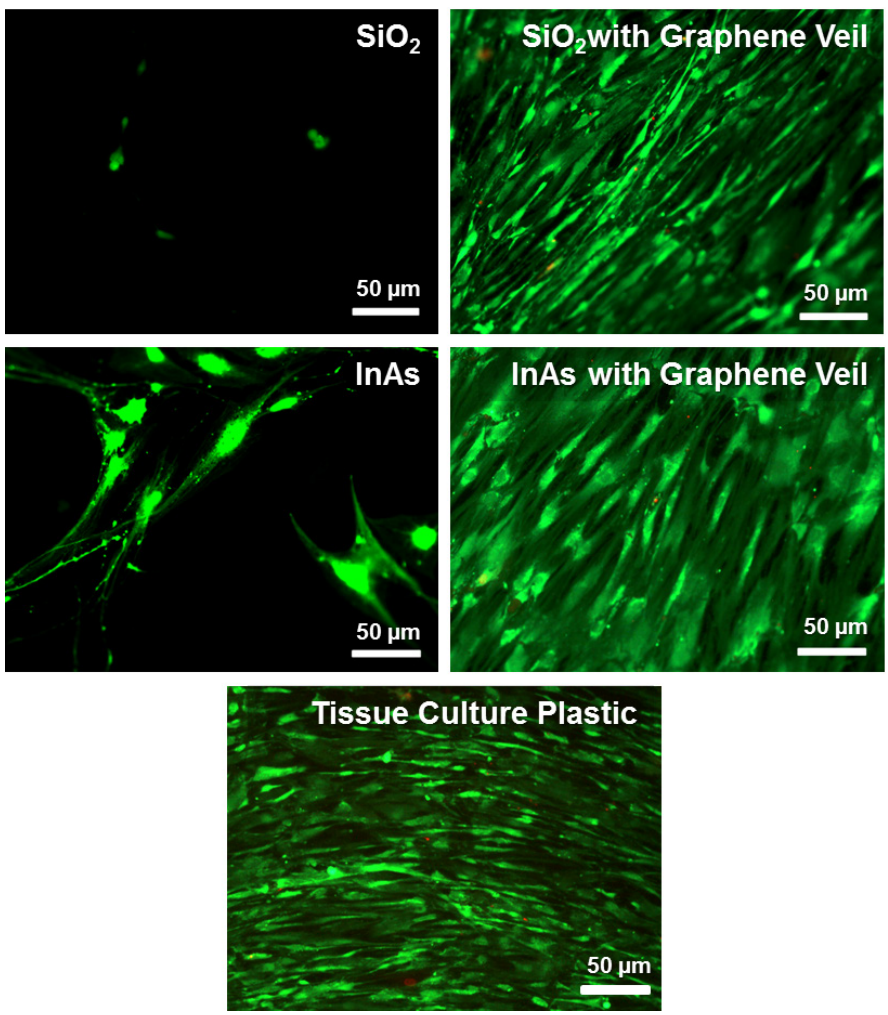

Figure 3. Fluorescence live/dead images of human mesenchymal stem cells grown atop SiO_2 and InAs. Cells were grown on surfaces with and without a graphene veil coating. Also shown is the control surface, tissue culture plastic. Micrographs are a composite of live (green; calcein AM) and dead (red; EthD-1) stains.

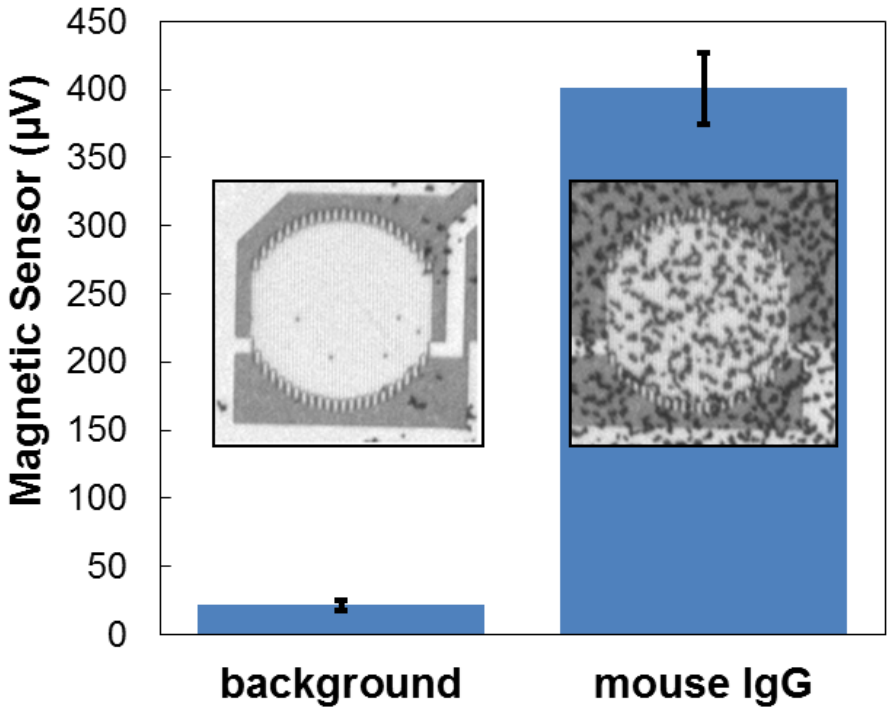

Figure 4. FFD immunoassay for detection of mouse IgG performed on a graphene veil coating a magnetic sensor chip. Bar graph depicts the average signal measured at five embedded magnetic sensors. The inlaid pictures show representative images of the graphene veil coated sensor chip.

background by removing nonspecifically bound beads but also requires a strong tethering to the substrate for the specifically bound beads. The reproducible and uniform distribution of beads in the positive results shown in Figure 2 is the clearest demonstration that the graphene veils do not delaminate; in addition, the excellent background in the negative control images make the same point since delamination would lead to nonspecific binding.

In addition to its ability to biofunctionalize a wide range of technologically important substrates, GO also enables the growth of living cells. Figure 3 demonstrates that graphene veils support the growth and function of human mesenchymal stem cells (hMSC), a fairly delicate class of cells (42,43). Shown are micrographs for hMSCs grown atop SiO_2 or InAs, either with or without a graphene veil coating. The fluorescence images show live (green) / dead (red) stained hMSCs on each substrate material and also a tissue culture plastic control surface after three weeks of growth. Healthy, confluent cell beds were observed atop the graphene veil, but almost no cells were attached to the substrate materials without the intermediary graphene veil. These results highlight a key to the graphene veil's generality; the film masks the substrate's surface properties from the attached biomolecules. This means that functionalization is only dependent on the biological entity interacting with the GO film, and the same surface chemistry can be applied to many different sensor substrates. Nowhere is this more important than in the graphene veil's ability to support cell growth and function. Cell compatibility with graphene surfaces is well known, with many reports in the literature (44–47). Here we demonstrate that sensor substrates that would otherwise be inhospitable for cell culture are viable choices if a graphene veil is used as an intermediary layer. This method potentially opens up a wide variety of new materials and transduction methods to in vitro studies.

Graphene veils' utility requires not only the functionalization of diverse sensing materials but also that the sensors can transduce with the veil in place. Figure 4 demonstrates the detection of mouse IgG antibody following a FFD assay performed atop a sensor chip with embedded magnetic field sensors. Magnetic based biosensing is a small, but burgeoning field, and the U.S. Naval Research Laboratory's *cBASS* system has demonstrated rapid, attomolar protein detection (48). The sensor chip for *cBASS* was coated with silicon nitride to prevent the magnetoresistive wires from shorting while in aqueous buffers. A graphene veil was cast atop the silicon nitride surface, then functionalized with NA using EDC/NHS coupling, and individual sensors were spotted with biotinylated capture antibody. The bar graph shown in Figure 4 depicts the average response from five antibody functionalized sensors for the detection of mouse IgG antibody. For comparison, the average signal at five sensors without capture antibody is given. Representative images of a bead covered sensor following FFD assays are inlayed to demonstrate the correlation between bead capture and the magnetic signal measured. Note that the thin design of the graphene veil makes this transduction possible. For magnetoresistive sensors, signal drops off as r^6 as the bead is separated from the substrate, so the thinnest coating possible is required to maximize signal (48).

Magnetoresistive sensors are just one of many sensor classes that depend critically on separation distance. For example, distance dependent transduction is observed for both bioFETS and SPR biosensors. It is well established that bioFETS are subject to Debye screening, which limits sensing to the first 10 nm above the sensor surface. Similarly, SPR sensors show a distance dependence of ~100 nm above the substrate (14). All 3 types of distance dependent sensors discussed are therefore accommodated by the thin, ~4 nm profile of the graphene veil. Literature also suggests that graphene veils are compatible with electrochemical and optical transduction methods. Carbon electrodes are well established for electrochemical measurements, and the conductivity of the aminated graphene veil can be established by reduction of the GO with hydrazine (35); importantly, the EDA functionalization is known to survive the reduction process.

Graphene veils are transparent in visible and near-IR wavelengths, meaning that optical transduction such as colorimetric and ELISA assays should be possible. Fluorescence detection has even been demonstrated atop graphene films by spacing the fluorophores further than the FRET quenching distance (49).

In conclusion, we have demonstrated that graphene veil coating of sensors is a versatile surface functionalization strategy for a wide range of bioassays. The thin films are inexpensive, easy to produce, and perform reproducibly independent of the substrate. We have coated five diverse sensor materials, including organic and semiconductor materials, to demonstrate the generality of the approach. Additionally, the SPR–graphene work discussed demonstrates that the approach can be expanded to metal films as well. This method delivers conformal coatings of sensor substrates. Graphene veils provide multiple reaction pathways for functionalization as shown by our attachment of peptides, antibodies, globular proteins, and DNA. The attached biomolecules were fully functional and bioavailable, allowing us to perform nucleic acid hybridization and immunoassays in both buffer and serum, showing no greater background accumulation in the latter as compared with optimized conventional chemistries that were substrate-dependent. The robust nature of the graphene veil was demonstrated by our choice of a mechanically demanding FFD assay. The reproducible and uniform distribution of beads in the images shown in Figure 2 is the clearest demonstration that the graphene veils do not delaminate and are well adhered to the surface. Finally, graphene veils expand the possibilities for in vitro studies by supporting cell growth and function on what would otherwise be inhospitable materials.

Author Contributions

All of authors collaborated to make possible the work presented in this manuscript. S.P.M. and P.E.S. conceived of and developed the graphene veils concept; R.S. contributed to graphene functionalization and patterning; C.R.T. contributed mechanical and fluidic engineering solutions; and N.L. performed microbiology.

Competing Interests

The authors declare no competing interests.

References

1. **Börsch, M.** 2011. Single-molecule fluorescence resonance energy transfer techniques on rotary ATP synthases. Biol. Chem. *392*:135-142.
2. **Liu, C., Y.Y. Qu, Y. Luo, and N. Fang.** 2011. Recent advances in single-molecule detection on micro- and nano-fluidic devices. Electrophoresis *32*:3308-3318.
3. **Treffer, R. and V. Deckert.** 2010. Recent advances in single-molecule sequencing. Curr. Opin. Biotechnol. *21*:4-11.
4. **Blaszykowski, C., S. Sheikh, and M. Thompson.** 2012. Surface chemistry to minimize fouling from blood-based fluids. Chem. Soc. Rev. *41*:5599-5612.
5. **Sapsford, K.E., W.R. Algar, L. Berti, K.B. Gemmill, B.J. Casey, E. Oh, M.H. Stewart, and I.L. Medintz.** 2013. Functionalizing Nanoparticles with Biological Molecules: Developing Chemistries that Facilitate Nanotechnology. Chem. Rev. *113*:1904-2074.
6. **Hvilsted, S.** 2012. Facile design of biomaterials by click' chemistry. Polym. Int. *61*:485-494.
7. **Mandler, D. and S. Kraus-Ophir.** 2011. Self-assembled monolayers (SAMs) for electrochemical sensing. J. Solid State Electrochem. *15*:1535-1558.
8. **Mout, R., D.F. Moyano, S. Rana, and V.M. Rotello.** 2012. Surface functionalization of nanoparticles for nanomedicine. Chem. Soc. Rev. *41*:2539-2544.
9. **Zhou, Y., C.W. Chiu, and H. Liang.** 2012. Interfacial Structures and Properties of Organic Materials for Biosensors: An Overview. Sensors (Basel). *12*:15036-15062.
10. **Samanta, D. and A. Sarkar.** 2011. Immobilization of bio-macromolecules on self-assembled monolayers: methods and sensor applications. Chem. Soc. Rev. *40*:2567-2592.
11. **Luo, X. and J.J. Davis.** 2013. Electrical biosensors and the label free detection of protein disease biomarkers. Chem. Soc. Rev. *42*:5944-5962.
12. **Petryayeva, E. and U.J. Krull.** 2011. Localized surface plasmon resonance: Nanostructures, bioassays and biosensing-A review. Anal. Chim. Acta *706*:8-24.
13. **Stine, R., B.S. Simpkins, S.P. Mulvaney, L.J. Whitman, and C.R. Tamanaha.** 2010. Formation of amine groups on the surface of GaN: A method for direct biofunctionalization. Appl. Surf. Sci. *256*:4171-4175.
14. **Mariani, S. and M. Minunni.** 2014. Surface plasmon resonance applications in clinical analysis. Anal. Bioanal. Chem. *406*:2303-2323.
15. **Zheng, L.Z., X. Yao, and J.H. Li.** 2006. Layer-by-layer assembly films and their applications in electroanalytical chemistry. Curr. Anal. Chem. *2*:279-296.
16. **Deshmukh, P.K., K.P. Ramani, S.S. Singh, A.R. Tekade, V.K. Chatap, G.B. Patil, and**

S.B. Bari. 2013. Stimuli-sensitive layer-by-layer (LbL) self-assembly systems: Targeting and biosensory applications. J. Control. Release *166*:294-306.

17. **Tan, C.P. and H.G. Craighead.** 2010. Surface Engineering and Patterning Using Parylene for Biological Applications. Materials. *3*:1803-1832.
18. **Turchanin, A., A. Beyer, C.T. Nottbohm, X.H. Zhang, R. Stosch, A. Sologubenko, J. Mayer, P. Hinze, et al.** 2009. One Nanometer Thin Carbon Nanosheets with Tunable Conductivity and Stiffness. Adv. Mater. *21*:1233-1237.
19. **Angelova, P., H. Vieker, N.E. Weber, D. Matei, O. Reimer, I. Meier, S. Kurasch, J. Biskupek, et al.** 2013. A Universal Scheme to Convert Aromatic Molecular Monolayers into Functional Carbon Nanomembranes. ACS Nano *7*:6489-6497.
20. **Schnietz, M., A. Turchanin, C.T. Nottbohm, A. Beyer, H.H. Solak, P. Hinze, T. Weimann, and A. Golzhauser.** 2009. Chemically Functionatized Carbon Nanosieves with 1-nm Thickness. Small *5*:2651-2655.
21. **Novoselov, K.S., A.K. Geim, S.V. Morozov, D. Jiang, Y. Zhang, S.V. Dubonos, I.V. Grigorieva, and A.A. Firsov.** 2004. Electric field effect in atomically thin carbon films. Science *306*:666-669.
22. **Guo, S.J. and S.J. Dong.** 2011. Graphene and its derivative-based sensing materials for analytical devices. J. Mater. Chem. *21*:18503-18516.
23. **Jiang, H.** 2011. Chemical Preparation of Graphene-Based Nanomaterials and Their Applications in Chemical and Biological Sensors. Small *7*:2413-2427.
24. **Singh, V.V., G. Gupta, A. Batra, A.K. Nigam, M. Boopathi, P.K. Gutch, B.K. Tripathi, A. Srivastava, et al.** 2012. Greener Electrochemical Synthesis of High Quality Graphene Nanosheets Directly from Pencil and its SPR Sensing Application. Adv. Funct. Mater. *22*:2352-2362.
25. **Wang, L., C.Z. Zhu, L. Han, L.H. Jin, M. Zhou, and S.J. Dong.** 2011. Label-free, regenerative and sensitive surface plasmon resonance and electrochemical aptasensors based on graphene. Chem. Commun. (Camb.) *47*:7794-7796.
26. **Choi, S.H., Y.L. Kim, and K.M. Byun.** 2011. Graphene-on-silver substrates for sensitive surface plasmon resonance imaging biosensors. Opt. Express *19*:458-466.
27. **Wu, L., H.S. Chu, W.S. Koh, and E.P. Li.** 2010. Highly sensitive graphene biosensors based on surface plasmon resonance. Opt. Express *18*:14395-14400.
28. **Stine, R. and D.Y. Petrovykh.** 2009. Oriented self-assembled monolayers of bifunctional molecules on InAs. J. Electron. Spectros. Relat. Phenomena. *172*:42-46.
29. **Nistor, R.A., M.A. Kuroda, A.A. Maarouf, and G.J. Martyna.** 2012. Doping of adsorbed graphene from defects and impurities in SiO2 substrates. Phys. Rev. B. *86*:041409.
30. **Shih, C.J., G.L.C. Paulus, Q.H. Wang, Z. Jin, D. Blankschtein, and M.S. Strano.** 2012. Understanding Surfactant/Graphene Interactions Using a Graphene Field Effect Transistor: Relating Molecular Structure to Hysteresis and Carrier Mobillity. Langmuir *28*:8579-8586.
31. **Slawinska, J., I. Wlasny, P. Dabrowski, Z. Klusek, and I. Zasada.** 2012. Doping domains in graphene on gold substrates: First-principles and scanning tunneling spectroscopy studies. Phys. Rev. B. *85*:235430.
32. **Guo, Z.X., J.W. Ding, and X.G. Gong.** 2012. Substrate effects on the thermal conductivity of epitaxial graphene nanoribbons. Phys. Rev. B *85*:235429.
33. **Hummers, W.S. and R.E. Offeman.** 1958. Preparation of Graphitic Oxide. J. Am. Chem. Soc. *80*:1339.
34. **Stine, R., J.T. Robinson, P.E. Sheehan, and C.R. Tamanaha.** 2010. Real-Time DNA Detection Using Reduced Graphene Oxide Field Effect Transistors. Adv. Mater. *22*:5297-5300.
35. **Stine, R., J.W. Ciszek, D.E. Barlow, W.K. Lee, J.T. Robinson, and P.E. Sheehan.** 2012. High-Density Amine-Terminated Monolayers Formed on Fluorinated CVD-Grown Graphene. Langmuir *28*:7957-7961.
36. **Mulvaney, S.P., C.L. Cole, M.D. Kniller, M. Malito, C.R. Tamanaha, J.C. Rife, M.W. Stanton, and L.J. Whitman.** 2007. Rapid, femtomolar bioassays in complex matrices combining microfluidics and magnetoelectronics. Biosens. Bioelectron. *23*:191-200.
37. **Mulvaney, S.P., K.M. Myers, P.E. Sheehan, and L.J. Whitman.** 2009. Attomolar protein detection in complex sample matrices with semi-homogeneous fluidic force discrimination assays. Biosens. Bioelectron. *24*:1109-1115.
38. **Ji, G., B. Ding, Z. Sha, J.S. Wu, Y. Ma, and J.Y. Lee.** 2013. Conformal graphene encapsulation of tin oxide nanoparticle aggregates for improved performance in reversible Li+ storage. Nanoscale. *5*:5965-5972.
39. **Dai, Y.Q., Y. Jing, J. Zeng, Q. Qi, C.L. Wang, D. Goldfeld, C.H. Xu, Y.P. Zheng, and Y.M. Sun.** 2011. Nanocables composed of anatase nanofibers wrapped in UV-light reduced graphene oxide and their enhancement of photoinduced electron transfer in photoanodes. J. Mater. Chem. *21*:18174-18179.
40. **Bruus-Jensen, K., T. Poethko, M. Schottelius, A. Hauser, M. Schwaiger, and H.J. Wester.** 2006. Chemoselective hydrazone formation between HYNIC-functionalized peptides and F-18-fluorinated aldehydes. Nucl. Med. Biol. *33*:173-183.
41. **Staros, J.V., R.W. Wright, and D.M. Swingle.** 1986. Enhancement by N-Hydroxysulfosuccinimide of Water-Soluble Carbodiimide-Mediated Coupling Reactions. Anal. Biochem. *156*:220-222.
42. **Vallone, V.B.F., M.A. Romaniuk, H. Choi, V. Labovsky, J. Otaegui, and N.A. Chasseing.** 2013. Mesenchymal stem cells and their use in therapy: what has been achieved? Differentiation. *85*:1-10.
43. **Lin, C.S., Z.C. Xin, C.H. Deng, H.X. Ning, G.T. Lin, and T.F. Lue.** 2010. Defining adipose tissue-derived stem cells in tissue and in culture. Histol. Histopathol. *25*:807-815.
44. **Chung, C., Y.-K. Kim, D. Shin, S.-R. Ryoo, B.H. Hong, and D.-H. Min.** 2013. Biomedical Applications of Graphene and Graphene Oxide. Acc. Chem. Res. *46*:2211-2224.
45. **Ku, S.H., M. Lee, and C.B. Park.** 2013. Carbon-Based Nanomaterials for Tissue Engineering. Adv. Healthc. Mater. *2*:244-260.
46. **Yang, M., J. Yao, and Y. Duan.** 2013. Graphene and its derivatives for cell biotechnology. Analyst. *138*:72-86.
47. **Pryzhkova, M.V.** 2013. Concise Review: Carbon Nanotechnology: Perspectives in Stem Cell Research. Stem Cells Trans.l Med. *2*:376-383.
48. **Tamanaha, C.R., S.P. Mulvaney, J.C. Rife, and L.J. Whitman.** 2008. Magnetic labeling, detection, and system integration. Biosens. Bioelectron. *24*:1-13.
49. **Huang, P.J.J. and J.W. Liu.** 2012. DNA-Length-Dependent Fluorescence Signaling on Graphene Oxide Surface. Small *8*:977-983.

Received 13 March 2014; accepted 04 June 2014.

Address correspondence to Shawn P. Mulvaney, US Naval Research Laboratory, Washington, DC. E-mail: shawn.mulvaney@nrl.navy.mil